



Groundwater contamination monitoring and modeling for a part of Satluj River basin

Akshay Kumar Chaudhry^{a,*}, Mohammad Afaq Alam^b, Kamal Kumar^c

^aResearch Scholar, Department of Civil Engineering, Punjab Engineering College (Deemed to be University), Chandigarh, India, email: akki016@gmail.com

^bAssociate Professor, Department of Civil Engineering, Punjab Engineering College (Deemed to be University), Chandigarh, India, email: afaqalam@pec.ac.in

^cAssistant Professor, Department of Civil Engineering, Punjab Engineering College (Deemed to be University), Chandigarh, India, email: kamalkumar@pec.ac.in

Received 3 April 2020; Accepted 24 September 2020

ABSTRACT

Owing to growing urbanization, industrialization, and rise in agronomic development, the Rupnagar district of Punjab had been under stress by groundwater pumping during the past decade. The area has recently seen a substantial decrease in the water level of various boreholes and wells, and a major degradation in groundwater quality due to salinization (increase in total dissolved solids [TDS]). Leakage from some industries in the region might be a contamination source that would threaten groundwater quality. Thus, models for groundwater flow (MODFLOW) and particle tracking (mod-PATH3DU) for two periods, at the present (2020) and 10 y prediction (2030) were used to determine groundwater flow patterns, principal groundwater discharge and recharge zones, and estimates of groundwater travel-times in the region. Based on sensitivity analysis, it was observed that changes in hydraulic conductivity will boost flow patterns within the region, mainly because it contributes to the homogenization of flow and removes low-volume zones. Ten years prediction indicated that TDS tends to move from the topsoil to the deeper aquifer. The plume migration would not exceed 10 km in radius from all the sources and is considered to be a slow process. Consequently, both long-term observations and simulations showed that concentrations of TDS in the receiving waters are positively correlated with the intensity of urbanization and industrialization. Besides, rehabilitation of contaminated sites should be undertaken to prevent further mobilization of contaminants.

Keywords: Groundwater contamination; MODFLOW; mod-PATH3DU; Numerical modeling; TDS; Remediation

1. Introduction

Groundwater quality plays a key role in the sustainable development and management of water resources. Groundwater salinization is one of the key causes of a decline in the consistency of groundwater [1,2]. It is one of the fast-growing problems in the world, caused by an increase in total dissolved solids in water (TDS) due to natural or various anthropogenic causes [3]. It is a chemical process that leads to the degradation of arable soil, desertification, and reduction of biomass; therefore, monitoring the progress of this process is essential for the

preparation of measures to protect at-risk regions [4]. The sources and processes involved in the salinization of inland and coastal aquifers vary. Additionally, the salinity of the freshwater aquifers can also be increased if the saltwater and freshwater mix in the subsurface. The salinity of any region depends on the intensity and distribution of precipitation and evapotranspiration, rate of recharge, the aquifer material types and its characteristics, the residence time, the flow rate, and the nature of the discharge areas [5,6]. However, the main mechanisms that control changes in salinity over time and space need to be identified in order to identify sources of salinization.

Historically, geophysical approaches have been used to describe possible contaminant migration pathways.

* Corresponding author.

Details regarding various geophysical methods used for tracking the groundwater contaminant over time can be found out in this literature [7]. With the development of accurate, flexible, and reliable groundwater models, the use of certain geophysical methods now is limited mainly by the lack of interpretation capability [8]. Thus, numerical modeling plays an important role in the real-life management of groundwater systems from contamination. Groundwater models are the backbones of water resource planning and management in arid and semi-arid regions [9]. Different methods have been developed so far to investigate groundwater flow and contaminant transport [10–20]. Bachmat et al. [21] in his review article listed a total of 177 flow and mass transport models along with their applications in groundwater management. Abriola [22,23] reported advanced articles related to solute transport modeling in groundwater. In this study, MODFLOW [24] and MODPATH3DU (extension of MODPATH) [25] were used as numerical modeling tools. Previous studies on MODFLOW and MODPATH showed that they are reliable tools in simulating the groundwater flow and particle movement [26,27].

There has been a paradigm shift from “groundwater development” to “groundwater quality management” in the past decade in the study region. The most important factors, which decrease the groundwater quality, are salinization, rapid industrialization, urbanization, excessive pumping for agronomic activities, and increase in anthropogenic sources in the region [28]. Major anthropogenic causes include irrigation of dry areas with a lack of adequate drainage, increased evaporation and decreased precipitation due to climate change, wastewater with a high salt content being carefully disposed of by industries on the surface, leading to salinization in the region [6,29–32]. In April 2016, the Punjab Pollution Control Board (PPCB) came out with a report, post-testing water quality from 37 locations where the Satluj River flows in the state. The river, which enters the study region, begins to deteriorate as it runs its course in the state [33]. The PPCB and Central Groundwater Board (CGWB) are the water bodies working under Punjab Government and Ministry of India, respectively, to preserve the wholesomeness of water in the region. They monitor the region to study the effect on water quality due to various effluents/wastewater discharge. The government has made many efforts to establish several sewage treatment plants (STPs) in the concerned area along with regular groundwater monitoring to ensure that no untreated sewage/effluent from industries and STPs may affect the quality of water in the region. Yet, the TDS concentration of groundwater has reached about $\geq 1,000$ mg/L at some of the source locations in the study region as a result of natural and human activities [34,35]. In general, the concentration of TDS in the area tends to be associated with local lithology. The spatial discontinuity of the TDS plumes in the flow domain has also been noted. This may be due to the presence of clay patches. The stage of groundwater development in the region reached up to $\cong 110\%$, which puts it in the overexploited category. Therefore, the industries and the vast population of the area need a significant quantity of water, most of which is supplied by groundwater abstraction. Thus, specific objectives of this study were to elucidate groundwater flow patterns, which includes

identification of principal groundwater recharge and discharge zones; identify potential time scales for TDS contamination to affect the area, and to address management implications of model results with respect to groundwater TDS loading to surface water. To the best of our knowledge, no such study has been conducted previously in the region to efficiently address source-based salinization. All the simulations in this study are carried out using Visual MODFLOW Flex 6 Software.

2. Study area and data procurement

Rupnagar district, Punjab ($76^{\circ}16'26''\text{E}$ - $76^{\circ}43'21''\text{E}$, $30^{\circ}44'21''\text{N}$ - $31^{\circ}25'53''\text{N}$) is a part of Indo-Gangetic basin and is located in the eastern part of the Punjab State. It covers an area of $1,414$ km² (Figs. 1a and b). Agriculture is an important source of economy in the state covering almost 55% of the area. The main crops grown are rice, maize, wheat, and vegetables. Most of the fallow and uncultivated land is barren with few shrubs and bushes. The geological map of the area has been prepared taking into account the previous geological investigations [36,37]. The study area is covered with quaternary sediments, mainly of fluvial nature. Newer alluvium, older alluvium, upper and lower shiwaliks are the major geological units in the area (Fig. S1). The rock formations ranging in age from Pleistocene to recent are exposed. River Satluj is the chief source of water in the area. The climate here is semi-arid, with warm summers and cold winters. The district gets its rainfall through southwest monsoon, which contributes to about 78% of the total rainfall. In most of the regions, surface water bodies amalgamate during the monsoon. During the non-monsoon season, River Satluj, small distributaries, lakes, and ponds in the region dominate the surface hydrology. The general direction of groundwater in the northern part of the district is towards the south and south-easterly direction, whereas in the south-eastern part of the district the flow is in the south and south-western direction. The hydraulic gradient is gentle near the plains and steeper near the hills. Soil consists predominantly of four main types of soil, namely, ustochrepts, ustorthents, ustipsamments and ustifluvents [37], and water level fluctuations do not reflect the presence of numerous or distinct aquifer systems up to a depth of 200 m from the usual ground level. Though, based on the water withdrawal patterns, the alluvium deposits may be distinguished vertically as shallow, intermediate, and deep aquifers. The long-term trend of water level (17 y) shows a general decline in the entire district. The typical pattern of fluctuations in water levels in the calendar year is a decreasing trend from January to May, an increasing trend from June to September, and then a decline from October onwards. The mean pre- and post-monsoon groundwater levels range from 2.48–18.81 and 2.30–18.49 mbgl (meter below ground level), respectively. The hydrogeochemistry of the study region is described in a companion paper [38]. The transmissivity and hydraulic conductivity values reported from pumping tests conducted by CGWB range from 55 to $1,180$ m²/d and 3 to 48 m/d respectively. The storativity value ranges between 7.8×10^{-4} and 1.2×10^{-3} indicating semi-confined to confined conditions [39].

3. Methodology

3.1. Modeling approach (numerical model)

A three-dimensional (3-D), finite-difference groundwater flow models (constant-density) coupled with transport model (linear isotherm, equilibrium controlled) were constructed using the MODFLOW, and MT3DMS, respectively [24,40]. Development of the numerical models involved (1) formulation and evaluation of various spatial and temporal discretization schemes; (2) specification of initial and boundary conditions; (3) weighting of calibration heads and head differences; (4) model calibration and sensitivity analysis using the inverse method; and (5) particle-tracking simulations to visualize the 3-D flow and to assess model-derived groundwater flow paths, travel-times, and source areas for consistency with other independent lines of evidence. mod-PATH3DU particle tracking code was used for calculating the 3-D flow path lines and travel-times of solute particles [25]. It uses two different tracking schemes (Pollock and SSP&A method). In the present study, the Pollock method was used (Fig. 2). Detailed explanation, limitations, and the presentation of all the equations of this method are rather complex, the reader should refer to Pollock [41,42] and Lu [43] for details and are not written here for brevity.

3.2. Initial and boundary conditions

The boundary conditions are a key part of the groundwater flow model conceptualization. The model domain was spatially discretized using 40 rows, 30 columns, and

2 layers. The degree of vertical anisotropy was not well-known. Rainfall is the major source of groundwater recharge in the region. Precipitation recharge was allocated to model layer one cells at a uniform constant rate of 775 mm/y. Precipitation recharge was simulated as constant because it composes a small proportion of the water budget; most of the changes in water levels are related to precipitation in the tributary basins rather than to precipitation on the plain [44]. Similarly, evapotranspiration was allocated to model layer one cells at a uniform constant rate of 1,260 mm/y [45]. Major sinks include extraction wells for agricultural and municipal water supply. No-flow boundaries were imposed on the bottom faces of the aquifer system and the top is a steady-state prescribed head everywhere at the surface. The western and eastern boundaries are a no-flow due to impermeable hills in these locations. Constant head boundaries, which match the observed hydraulic heads in the area, were applied on the north and south sides. The boundaries at the major river are open to lateral groundwater flow (constant hydraulic head along the vertical boundary) [46]. The river in the simulation was represented by a group of nodes having head equal to the river stage and an average depth of 10 m. In order to determine well characteristics, estimation of aquifer parameters was carried out by CGWB by using pumping tests on wells (17 observation wells used in the study) at different locations (Table S1). In Table 1 we have shown those values that are applicable for the study region and are obtained from CGWB. The same aquifer properties were given to the model to simulate the groundwater fluxes across the study area. The process of

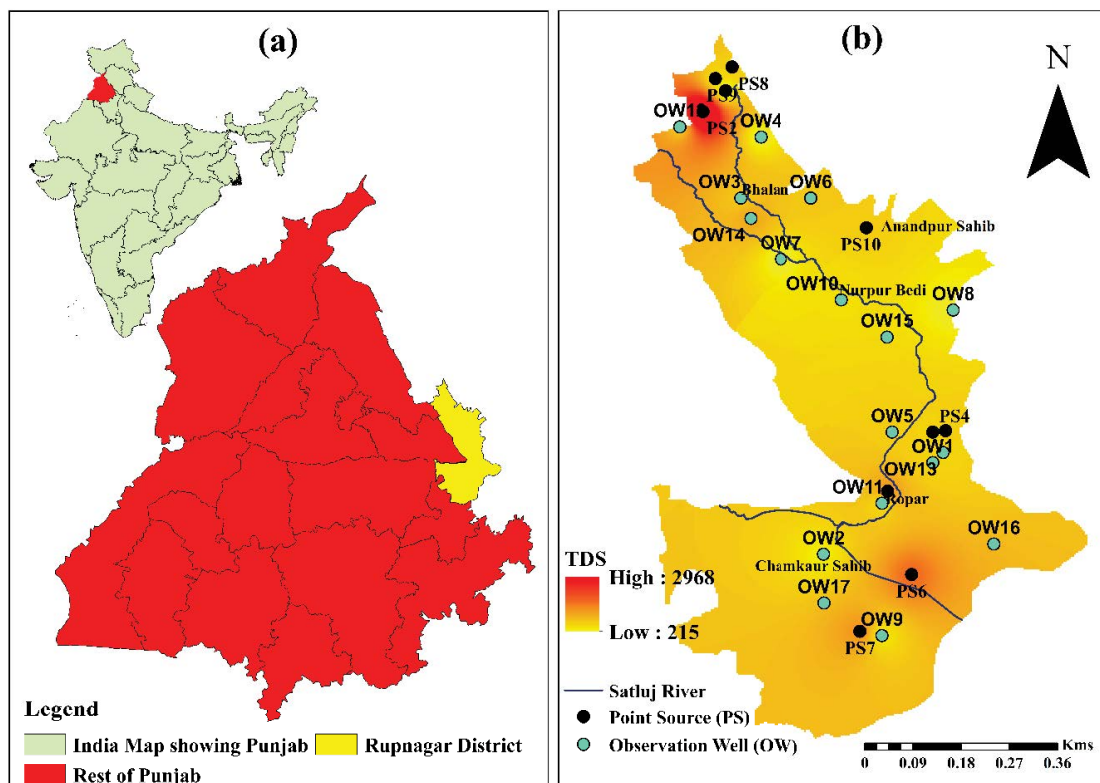


Fig. 1. (a) Location map of the study region; (b) observation wells, point sources, and TDS distribution in the study region.

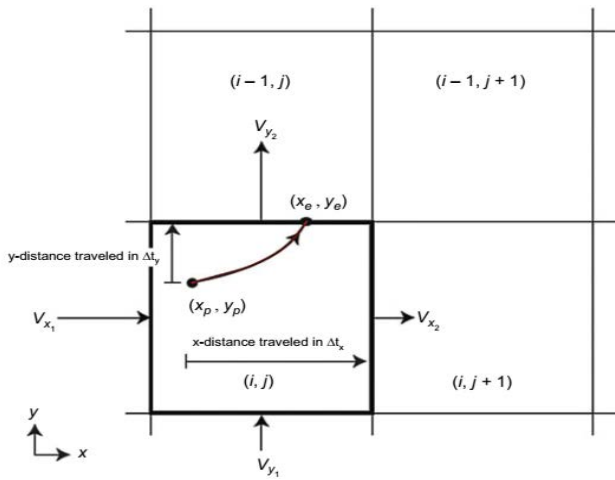


Fig. 2. Particle-tracking within a finite-difference cell/element showing the computation of flow path line and travel-time from the particle location (x_p, y_p) to an exit point (x_e, y_e) (Source: Pollock [41]).

contaminant injections was simulated as a specified flow boundary (Neumann) using the well module (located at layer 1). To solve the flow equation, the Block-Centered Flow Module (BCF) was applied. The BCF measures the flow components between adjacent cells and the component flow released and/or stored in the system, assuming the nodes situated at the center of each cell [47]. The algebraic equations were solved using the preconditioned conjugate gradient method (PCG2) [48], which addresses matrix equations if the matrix is symmetrical and positive-definite. All boundary conditions are defined regularly and are divided into 10 calculation steps per day to meet the convergence criteria [49].

4. Results and discussion

4.1. Groundwater flow simulation

For steady state (2010), the model simulated the hydraulic head distribution of 17 observation wells (Table S1) across the study region (Fig. 3a), with the correlation coefficient value of 0.92, and the normalised residual mean squared (RMS) value of 14.60%. For transient-state (i.e., 5,

10, and 15 y), the model simulated the hydraulic head distribution with the correlation coefficient value of 0.88, 0.87, and 0.85, respectively (Figs. 3b–d). In general, the magnitude and direction of the model-calibrated heads are slightly higher than the observed heads for both steady as well as transient-state. The goodness of the observed groundwater heads occurred in the regions with flat hydraulic gradients, while in the regions with a steeper hydraulic gradient the observed groundwater heads were poorly fit.

4.2. Model calibration and validation (sensitivity analysis)

The model in this study was calibrated by adjusting aquifer properties, by using an inverse method (i.e., parameter estimation tool [PEST]) [50]. The steady-state simulation was initially performed in model calibration to calibrate values of hydraulic conductivity in the defined zones using the highest recharge and the corresponding heads observed at the observation wells as initial inputs to the transient simulation. Steady-state calibration aimed at assisting a smooth convergence of the model and decreasing the global residual head in transient simulation [51]. The numerical model was calibrated when the flow budget and hydraulic head approximated the conditions specified in the project and additionally when the percentage difference between the flow and the outflow was less than 1% [52]. During the sensitivity analysis, it was observed that the model was highly sensitive to hydraulic conductivity and vertical anisotropy (VAN), the ratio of horizontal to vertical hydraulic conductivity. When hydraulic conductivity was tested, all the other parameters were kept constant. Measured head values of 17 observation well and TDS values of point sources were taken as initial guess values for sensitivity analysis. During sensitivity analysis, we assumed the hydraulic conductivity of the study region to be isotropic ($K_x = K_y = K_z$). This assumption provided the best calibration to observations of hydraulic head. Increase in VAN ($K_x:K_y = 5$ and 10) produced a poorer-fit to field data, increasing the normalized RMS of the hydraulic head to 17.85% and 20.47%, respectively (Fig. 4b and c). Several statistical measures (residual mean, normalised RMS, absolute residual mean, correlation coefficient, and root mean squared) were used to validate the same and the results are shown in Fig. 4a–f for head data, and Fig. 5a–c for TDS

Table 1
Model parameters values [39]

Model properties	Value
Hydraulic conductivity in longitudinal direction (K_x m/d)	13.00
Hydraulic conductivity in lateral direction (K_y m/d)	12.10
Hydraulic conductivity in vertical direction (K_z m/d)	1.30
Specific yield (S_y)	0.072
Effective porosity (n)	0.25
Total porosity	0.45
Transmissivity (m^2/s)	0.00064
Specific storage (S_s ; 1/m)	0.0003
Initial pollutant concentration (mg/L)	0.00

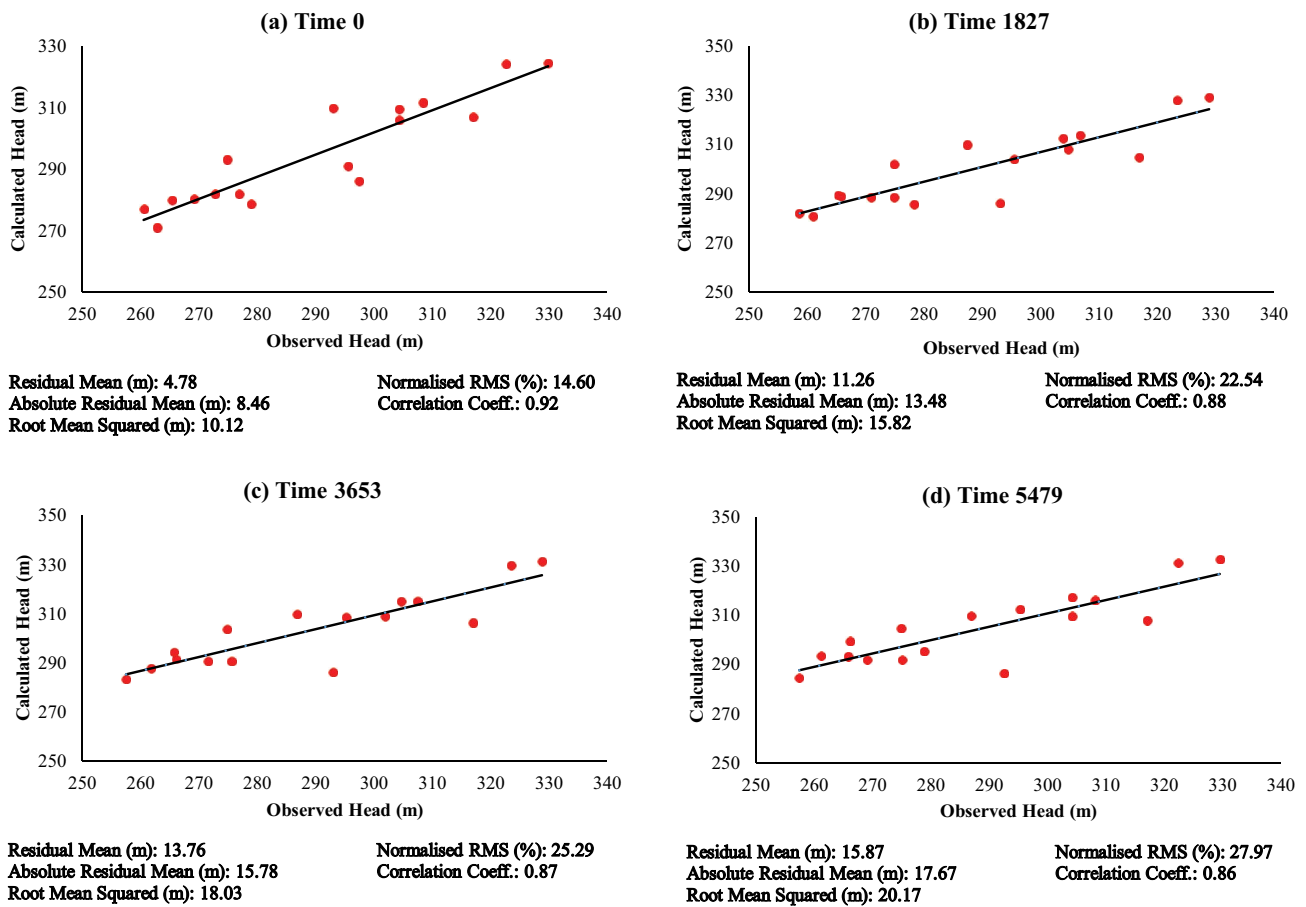


Fig. 3. (a) Steady-state head distribution before sensitivity analysis; (b–d) Transient-state head distribution for 5, 10, and 15-y stress period, respectively, before sensitivity analysis.

concentration data for VAN = 1 various hydraulic conductivity values were used to study the effect on head and TDS concentration. It was observed that increase in VAN. Model results revealed that groundwater flow is consistent with the previous interpretations of site hydrology. The general flow direction in the northern part of the district is towards the south and south-easterly direction whereas in the south-eastern part of the district the flow is in the south and south-western direction. Thus, the validated model was made to run for every year during the stress period. The results of the simulation process showed the predicted hydraulic head values for 5, 10, and 15 y with a correlation coefficient value of 0.97, 0.96, and 0.95, respectively.

4.3. Contaminant transport simulation

After the sensitivity analysis, the model was used to predict future contaminant conditions. Transport simulations were based on the concept of the previous transient model employing the MT3DMS module of mass transport [54]. In this study, the proposed transport model is non-reactive. The longitudinal (α_L) and two transverse directions (α_{TY} and α_{TZ}) dispersivity was assumed to be 50, 5, and 0.05 m, respectively [55]. The initial TDS concentration of 17 observation wells for the year 2010 was assigned. From the

results, it was elucidated that, TDS particles tend to move from the topsoil to the deeper depth. The horizontal distance does not expand while the vertical distance goes further down. The combined effect of the hydrodynamic dispersion coefficient due to water circulation and the natural flow direction renders the punctual contaminated zones slightly widened. The results of the simulation process showed the predicted concentration values for 5, 10, and 15 y with a correlation coefficient value of 0.99, 0.98, and 0.97 respectively (Figs. 5a–c). The computed iso-concentration TDS contours showed negligible contaminant transport for 15 y of transient transport runs and indicate that the plume is expanding (slow process) and follows the hydraulic gradient implying that advection is the dominant mechanism of spreading (Figs. 5d and e). From the aforementioned figure results, it can be elucidated that the frequency of salinization at one position does not have any effect on the transport of salinization from other pockets, but is due to in-situ activation. For all the point sources for the given input condition, the zone of influence is found to be in the order of 2 km from the release point. On the other hand, there is lateral flow starting after 20 y that threatens a great part of the city. The results of this analysis suggest that the main sources responsible for TDS salinization in the region are natural sources (i.e., carbonate

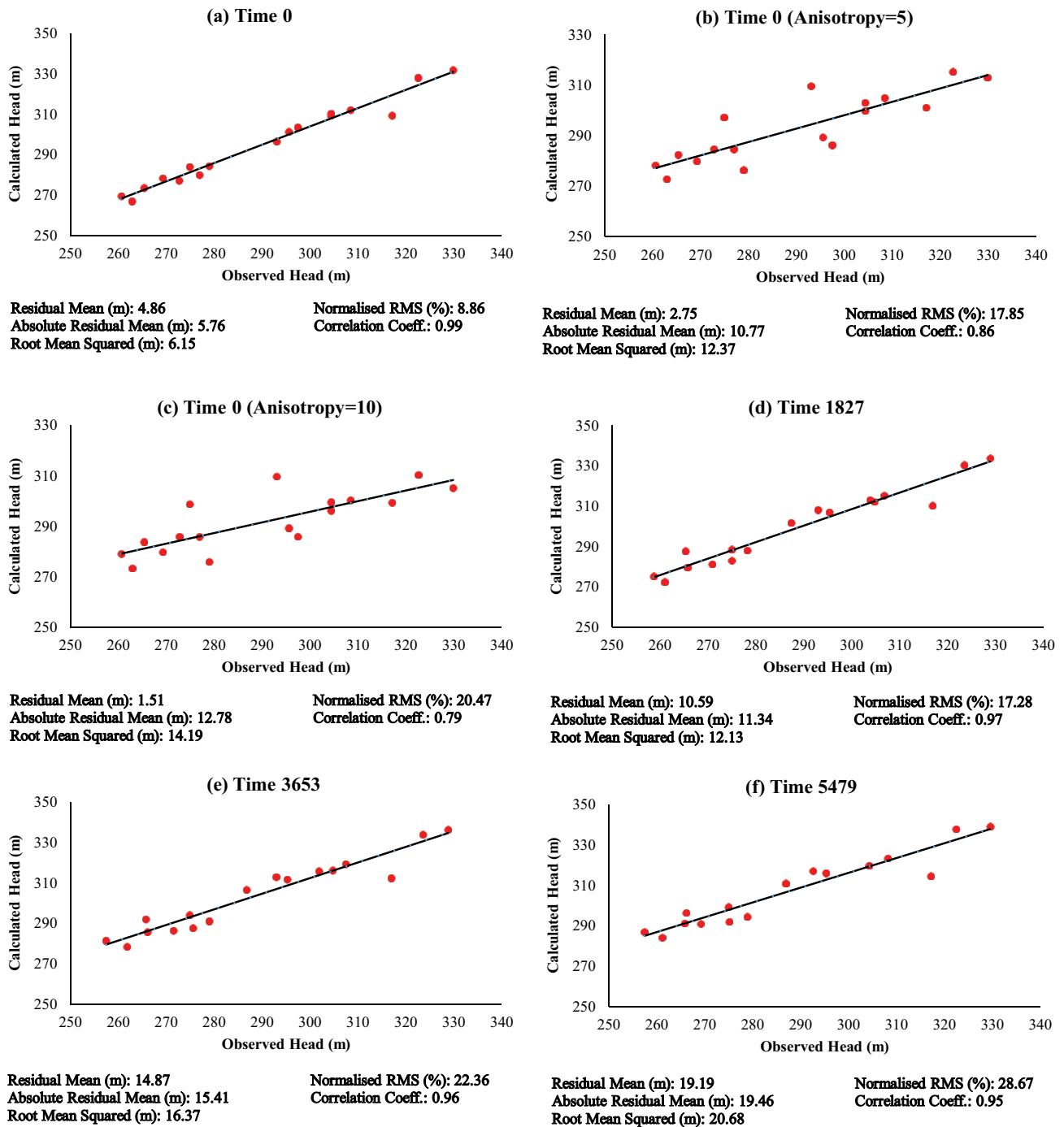


Fig. 4. (a) Steady-state head distribution after sensitivity analysis (with anisotropy = 1); (b and c) Steady-state head distribution before sensitivity analysis with varying anisotropy (d–f) Transient-state head distribution after sensitivity analysis (with anisotropy = 1) for 5, 10, and 15-y stress period, respectively.

and salt deposits), depleting water table, untreated raw sewage effluent, industrial wastewater, chemicals used in water treatment processes, coal burning, solid waste dumping grounds, and advance agronomic activates [39,56,57]. Natural systems, such as rivers, streams, and other water sources associated with the aquifer, have low TDS concentrations.

Direct impacts of flooding on the fate of contaminants have been reported, especially on their transportation between the environmental compartments of the atmosphere, water, soil, sediment, and biota (Alava et al. [58]). This occurs through physical, chemical, and biological processes, including possible dilution, concentration, and bifurcation of contaminants (Su et al. [59]). In addition,

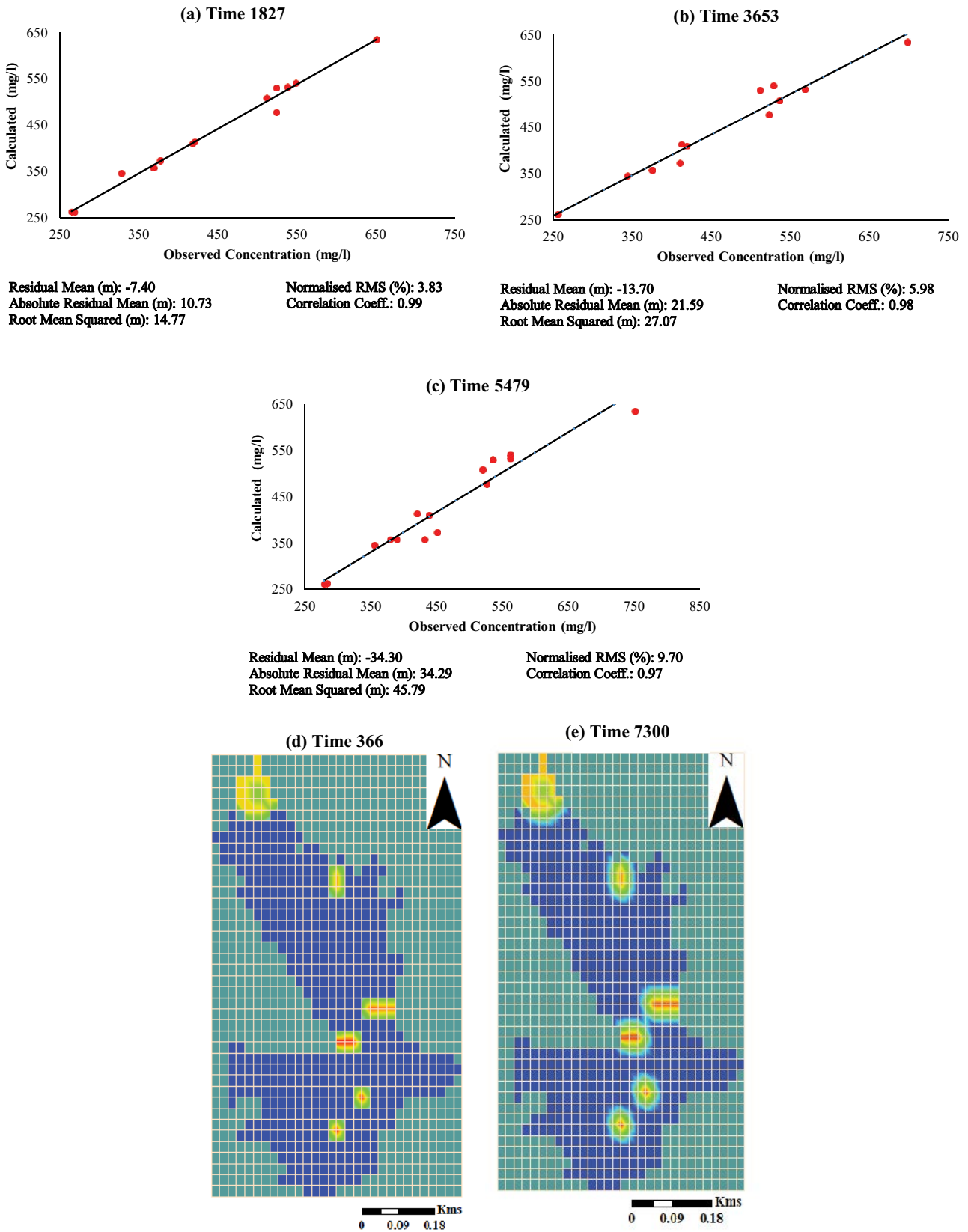


Fig. 5. (a–c) Calibrated transient-state head distribution (with anisotropy = 1) for 5, 10, and 15-y stress period, respectively; (d–e) Computed iso-concentration of TDS (mg/L) in the groundwater for 366 and 7,300 d, respectively.

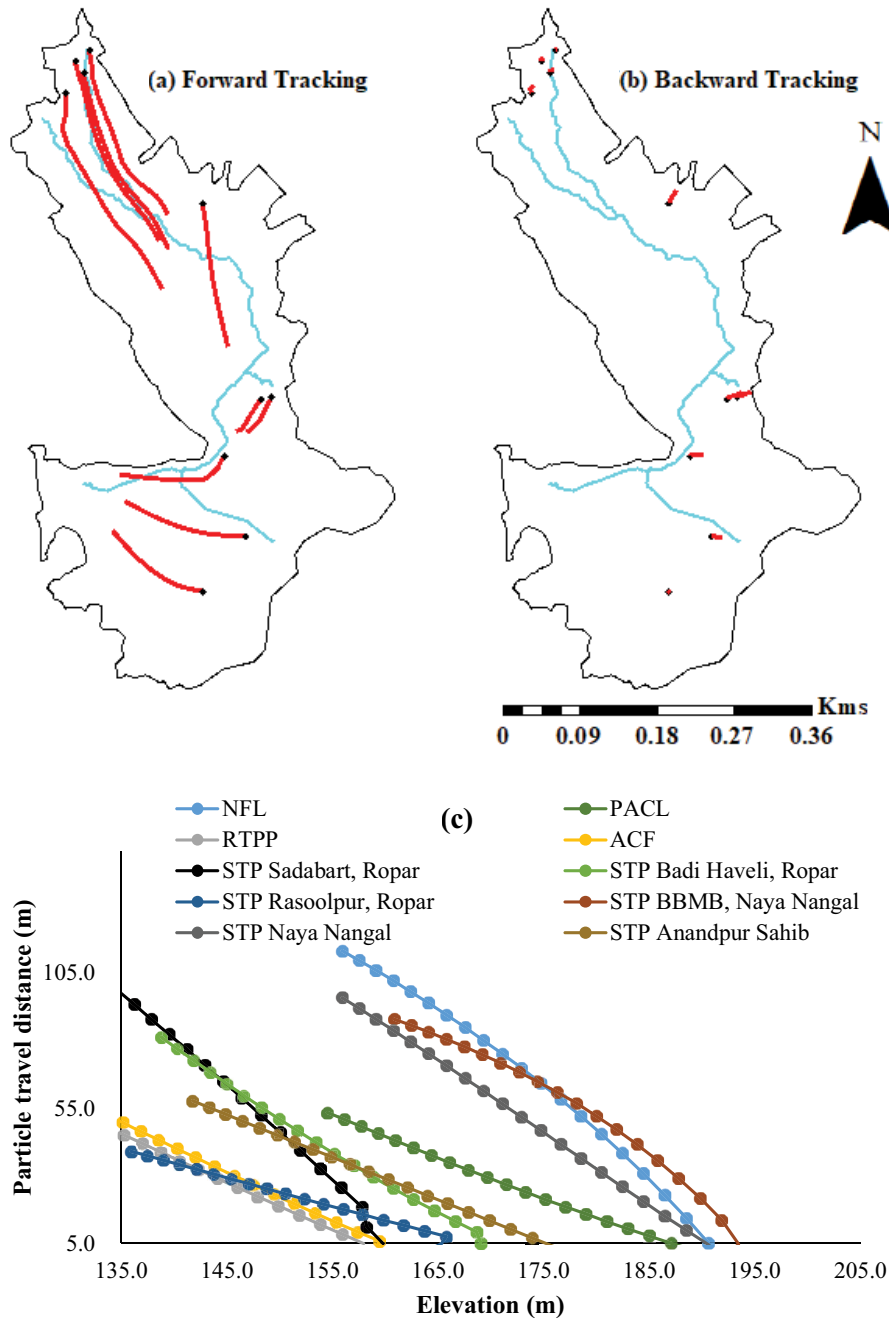


Fig. 6. (a and b) Forward (500 y) and backward particle (20 y) tracking; (c) plot showing decrease in particle travel distance with increase in elevation.

flooding can cause change in surface runoff, air-surface exchange, wet and dry deposition, dissolution by rain, and the transformation of contaminants.

4.4. Flow paths and travel-times

Particles (as a point) were assigned at all the point sources and were tracked forward and backward to the point of exit, thus, each particle approximating 1/10 of the total recharge to the flow system [60]. The resulting path lines along with the travel-times are shown (Figs. 6a

and b). These model computed travel-times do not account for the time required for water to travel from soil surface to the water table. Added to the model estimates, the migration of the particle from the surface of most of the sources is short and does not exceed 1.3 km after 20 y and can be considered a slow process. The length of path lines is proportional to the velocity of groundwater flow to a well field. It was observed that the particle travel distance was inversely proportional to the elevation (Fig. 6c). Additionally, the particle path lines distance of all the point sources for different stress periods are listed in Table 2.

Table 2
Particles travel distance for different stress period

Point source	Travel time (d)	1,825	3,650	5,475	7,300	10,950	14,600	18,250
PS1	FTD (m)	112.00	402.50	826.85	1,356.75	2,683.86	4,362.82	6,393.55
	BTD (m)	59.57	235.60	559.70	1,080.38	2,804.20	5,460.13	9,047.75
PS2	FTD (m)	39.10	145.52	320.18	561.75	1,244.22	2,196.68	3,419.07
	BTD (m)	44.18	166.75	370.44	656.44	1,475.83	2,625.24	4,104.59
PS3	FTD (m)	59.79	204.81	430.40	731.03	1,544.00	2,634.67	4,002.97
	BTD (m)	48.83	184.99	415.32	747.02	1,731.59	3,150.83	5,004.65
PS4	FTD (m)	63.79	213.82	446.32	755.47	1,583.23	2,688.13	4,070.11
	BTD (m)	49.43	187.81	421.94	757.78	1,752.81	3,187.20	5,060.86
PS5	FTD (m)	92.74	354.78	766.81	1,309.53	2,748.22	4,646.00	7,002.77
	BTD (m)	71.75	281.90	649.53	1,193.90	2,831.54	5,202.65	8,307.07
PS6	FTD (m)	65.94	235.39	512.27	897.17	1,988.40	3,507.96	5,455.76
	BTD (m)	68.90	254.71	557.80	977.69	2,175.94	3,842.61	5,977.60
PS7	FTD (m)	47.36	145.10	289.25	476.76	970.28	1,619.95	2,425.34
	BTD (m)	33.95	129.42	292.06	530.69	1,283.50	2,426.74	3,960.33
PS8	FTD (m)	104.80	363.79	721.90	1,149.78	2,172.23	3,413.31	4,872.96
	BTD (m)	40.80	162.57	393.82	786.15	2,164.69	4,363.57	7,382.61
PS9	FTD (m)	76.23	284.54	615.22	1,054.88	2,228.84	3,792.38	5,745.40
	BTD (m)	64.16	246.38	561.38	1,021.42	2,385.82	4,342.81	6,892.27
PS10	FTD (m)	51.21	179.52	378.47	642.46	1,357.93	2,213.88	3,532.76
	BTD (m)	43.73	165.37	371.60	670.04	1,558.82	2,839.96	4,502.38

FTD: Forward travel distance; BTD: backward travel distance.

5. Conclusion

In this study, we include one of the significant comparisons of groundwater data, showing that historical data can lead to advances within modeling the fate and transport of contaminants. Thus, TDS-contaminated groundwater in the study region has been analysed. A 3-D FDM model was conceptualised. The model was calibrated, validated, and simulated for flow paths and travel-time analysis of the contaminant (salinity) plume. The flow model perfectly demonstrated the flow paths and velocities with a high degree of precision. Simulations of several source alternatives conceptualisation established that salinization in the region is the result of localised in-situ sources, depleting water table, untreated raw sewage effluent, industrial wastewater, chemicals used in water treatment processes, coal burning, solid waste dumping grounds, and advance agronomic activities. There were no preferred flow paths in the river for plume migration during the initial years from the source locations, but it can occur in the near future. Contamination tends to move from the topsoil to the deeper aquifer. The migration would not exceed 10 km after 30 y and is considered a slow process. From the assumptions used in the study, it can be concluded that even with STPs in the region functioning to their full capacities, there is a possibility of further contamination to occur in the future if the present scenario continues. Thus, this study can act as a useful baseline data in the construction of more regional source-based groundwater models to prevent further mitigation of salinization in the region.

Further, to mitigate salinity in the region, these common practices should be adopted: improved irrigation practices; agroforestry and biological-drainage; mechanical reclamation; fractional wells; conjunctive water use; rehabilitation/replacement of saline groundwater wells; lining of water-courses in saline groundwater areas; rainwater utilization; and conservation tillage. There is no choice but to continue working towards salinity control. In the near future, we may expect some help from biotechnology for reclaiming salinized groundwater.

Lastly, the flow system modeled here is not unique. The combination of extensive pumping, a low topographic gradient, varying degrees of VAN, and countless sources of anthropogenic and natural groundwater contamination that bring about the water quality threat in the region can further help in contamination monitoring in the region and river deltas. Furthermore, contaminants may be retarded relative to the groundwater flow velocity or may be transformed by chemical processes. Such complexities were not considered in this analysis; and were beyond the scope of this work.

Acknowledgment

The authors wish to express our sincere gratitude to CGWB, Chandigarh, and PFCB, Mohali for providing the requisite data for this study.

Funding

This work received no particular grant from the government, private, or non-profit funding agencies.

References

- [1] A. Vengosh, Salinization and saline environment, *Treatise Geochem.*, 9 (2003) 1–35.
- [2] N. Gaaloul, L. Candela, A. Chebil, A. Soussi, K. Tamoh, Groundwater flow simulation at the Grombalia phreatic aquifer (Cap Bon, Northeastern Tunisia), *Desal. Water Treat.*, 52 (2013) 1997–2008.
- [3] N. Mokadem, B. Redhaouia, H. Besser, Y. Ayadi, F. Khelifi, A. Hamad, Y. Hamed, S. Bouri, Impact of climate change on groundwater and the extinction of ancient “Foggara” and springs systems in arid lands in North Africa: a case study in Gafsa basin (Central of Tunisia), *Euro-Mediterr. J. Environ. Integr.*, 3 (2018) 28.
- [4] N. Baghdadi, M. Zribi, Characterization of Soil Surface Properties Using Radar Remote Sensing. In: *Land Surface Remote Sensing in Continental Hydrology*, Elsevier, New York, 2016, pp. 1–39.
- [5] B.C. Richter, C.W. Kreitler, *Geochemical Techniques for Identifying Sources of Ground-Water Salinization*, CRC Press, 1993, p. 272.
- [6] K. Brindha, M. Schneider, Impact of Urbanization on Groundwater Quality, GIS and Geostatistical Techniques for Groundwater Science, 2019, pp. 179–196.
- [7] J.L. Osiensky, Time series electrical potential field measurements for early detection of groundwater contamination, *J. Environ. Sci. Health Part A*, 30 (1995) 1601–1626.
- [8] G.W. Hohmann, Numerical Modeling for Electromagnetic Methods of Geophysics, In: *Electromagnetic Methods in Applied Geophysics*, 1988, pp. 312–363.
- [9] R. Aghmand, A. Abbasi, Application of MODFLOW with boundary conditions analyses based on limited available observations: a case study of Birjand Plain in East Iran, *Water*, 11 (2019) 1904.
- [10] G. Sindhu, Effect of pumping on groundwater levels: a case study, *J. Inst. Eng. (India) Ser. A*, 99 (2013) 369–437.
- [11] A.N. Khondaker, R.I. Al-Layla, T. Husain, Groundwater contamination studies - the state-of-the-art, *Crit. Rev. Environ. Sci. Technol.*, 20 (1990) 231–256.
- [12] E.S. Bair, A.E. Springer, G.S. Roadcap, Delineation of traveltime-related capture areas of wells using analytical flow models and particle-tracking analysis, *Groundwater*, 29 (1991) 387–397.
- [13] N.Z. Sun, *Mathematical Modeling of Groundwater Pollution*, Springer, New York, 1996.
- [14] P.K. Majumdar, N.C. Ghosh, B. Chakravorty, Analysis of arsenic-contaminated groundwater domain in the Nadia district of West Bengal (India), *Hydrol. Sci. J.*, 4 (2002) S55–S66.
- [15] J.A. Izbicki, C.L. Stamos, T. Nishikawa, P. Martin, Comparison of ground-water flow model particle-tracking results and isotopic data in the Mojave River ground-water basin, southern California, USA, *J. Hydrol.*, 292 (2004) 30–47.
- [16] G. Kourakos, T. Harter, Vectorized simulation of groundwater flow and streamline transport, *Environ. Modell. Software*, 52 (2014) 207–221.
- [17] E.S. Bair, Applied Groundwater Modeling-Simulation of Flow and Advective Transport, *Groundwater*, 54 (2016) 756–757.
- [18] K.M. Ibrahim, A.R. El-Naqa, Inverse geochemical modeling of groundwater salinization in Azraq Basin, Jordan, *Arab. J. Geosci.*, 11 (2018) 237.
- [19] M.A. Sbai, A practical grid-based alternative method to advective particle tracking, *Groundwater*, (2018), doi:10.1111/gwat.12646.
- [20] X. Wu, J. Xia, C. Zhan, R. Jia, Y. Li, Y. Qiao, L. Zou, Modeling soil salinization at the downstream of a lowland reservoir, *Hydrol. Res.*, (2019), doi:10.2166/nh.2019.041.
- [21] Y. Bachmat, J. Bredehoeft, B. Andrews, D. Holtz, S. Sebastian, *Groundwater Management: the Use of Numerical Models*, Water Resources, Monograph: American Geophysical Union, 1980, p. 111.
- [22] L.M. Abriola, Modeling contaminant transport in subsurface - an interdisciplinary challenge, *Rev. Geophys.*, 25 (1987) 125.
- [23] L.M. Abriola, Modeling multiphase migration of organic chemicals in groundwater systems-a review and assessment, *Environ. Health Perspect.*, 83 (1989) 117–143.
- [24] A.W. Harbaugh, MODFLOW-2005, the U.S. Geological Survey Modular Ground-Water Model—The Ground-Water Flow Process, U.S. Geological Survey Techniques and Methods 6–A16, Reston, Virginia, USA, 2005.
- [25] C. Muffels, L. Scantlebury, X. Wang, M.J. Tonkin, C. Neville, M. Ramadhan, J.R. Craig, User's Guide for Mod-PATH3DU, A Groundwater Path and Travel-Time Simulator, S.S. Papadopoulos & Associates, Bethesda, MD, 2018.
- [26] M. Devi Nowbuth, P. Rambhojun, B. Umrikar, Numerical groundwater flow and contaminant transport modelling of the Southern Aquifer, Mauritius, *Earth Sci. India*, 5 (2012) 79–91.
- [27] H. Banejad, H. Mohebzadeh, M.H. Ghobadi, M. Heydari, Numerical simulation of groundwater flow and contamination transport in Nahavand Plain aquifer, west of Iran, *J. Geol. Soc. India*, 83 (2014) 83–92.
- [28] A.K. Chaudhry, K. Kamal, M.A. Alam, Spatial distribution of physico-chemical parameters for groundwater quality evaluation in a part of Satluj River Basin, India, *Water Supply*, 19 (2019) 1480–1490.
- [29] M. Mirzavand, H. Ghasemieh, S.J. Sadatinejad, R. Bagheri, An overview on source, mechanism and investigation approaches in groundwater salinization studies, *Int. J. Environ. Sci. Technol.*, (2020), doi:10.1007/s13762-020-02647-7.
- [30] S. Sharma, J. Kaur, A.K. Nagpal, I. Kaur, Quantitative assessment of possible human health risk associated with consumption of arsenic-contaminated groundwater and wheat grains from Ropar Wetland and its environs, *Environ. Monit. Assess.*, 188 (2016) 506.
- [31] Department of Science, Technology, and Environment (DSTE), Action Plan of Clean River Sutlej. Directorate of Environment and Climate Change: Punjab, India, 2019.
- [32] A. Sharma, In Ropar, Illegal Mining Takes Toll on Groundwater, (2019). Available at: <https://www.tribuneindia.com/news/punjab/in-ropar-illegal-mining-takes-toll-on-groundwater/802078.html> (Accessed: August 2020).
- [33] S. Dutta, The Degrading Water Quality of Sutlej, (2017). Available at: <http://swachhindia.ndtv.com/disposal-waste-grossly-polluting-industries-punjab-threaten-widely-used-rivers-state-12183/> (Accessed: August 2020).
- [34] P. Virk, N. Ghosh, K.P. Singh, Some trace elements investigation in groundwater around industrial belt of Ropar Block, Rupnagar District, Punjab, India, *J. Ind. Pollut. Control*, 26 (2010) 149–154.
- [35] Central Water Commission (CWC), Status of Trace and Toxic Metals in Indian Rivers, Ministry of Water Resources, India, 2018.
- [36] B. Singh, Regional Geochemical Mapping in Toposheet no 53A/4 district Nawanshahr and Hoshiarpur, Punjab, Geological Survey of India, New Delhi, Report No. NRO-21274, 2002.
- [37] A.K. Chaudhry, K. Kamal, M.A. Alam, Mapping of groundwater potential zones using the fuzzy analytic hierarchy process and geospatial technique, *Geocarto Int.*, (2019) 1–22.
- [38] A.K. Chaudhry, K. Kamal, M.A. Alam, Groundwater contamination characterization using multivariate statistical analysis and geostatistical method, *Water Supply*, 19 (2019) 2309–2322.
- [39] Central Groundwater Board (CGWB), Aquifer Mapping and Management Plan, Ropar District Punjab, Ministry of Water Resources, India, 2017.
- [40] V. Bedekar, E.D. Morway, C.D. Langevin, M. Tonkin, MT3D-USGS Version 1.0.0: Groundwater Solute Transport Simulator for MODFLOW, U.S. Geological Survey, Reston: Virginia, USA, 2016. doi: <http://dx.doi.org/10.5066/F75T3HKD>.
- [41] D.W. Pollock, Semi-analytical computation of path lines for finite-difference models, *Groundwater*, 26 (1988) 743–750.
- [42] D.W. Pollock, User Guide to MODPATH Version 7 – A Particle Tracking Model for MODFLOW, U.S. Geological Survey Open-File Report 2016–1086, 2016, p. 35.
- [43] N. Lu, A semianalytical method of path line computation for transient finite-difference groundwater flow models, *Water Resour. Res.*, 30 (1994) 2449–2459.
- [44] D.J. Ackerman, J.P. Rousseau, G.W. Rattray, J.C. Fisher, Steady-State and Transient Models of Groundwater Flow and Advective Transport, Eastern Snake River Plain aquifer, Idaho

- National Laboratory and vicinity, U.S. Geological Survey Scientific Investigations Report 2010–5123, Idaho, 2010, p. 220.
- [45] Central Water Commission (CWC), Sub-basin study under NWM- Appendix 2 Lower Sutlej Sub Basin, Ministry of Water Resources, India, 2011.
- [46] P. Sahu, H.A. Michael, C.I. Voss, P.K. Sikdar, Impacts on groundwater recharge areas of megacity pumping: analysis of potential contamination of Kolkata, India, water supply, *Hydrol. Sci. J.*, 58 (2013) 1340–1360.
- [47] M. Fioreze, M.A. Mancuso, MODFLOW and MODPATH for hydrodynamic simulation of porous media in horizontal subsurface flow constructed wetlands: a tool for design criteria, *Ecol. Eng.*, 130 (2019) 45–52.
- [48] M.C. Hill, Water-Resources Investigations Report 90–4048, In: Preconditioned Conjugate-Gradient 2 (PCG2), A Computer Program for Solving Ground-Water Flow Equations, USGS, 1990, p. 31.
- [49] B.F. Des Tombe, M. Bakker, F. Schaars, K.-J. van der Made, Estimating travel time in bank filtration systems from a numerical model based on DTS measurements, *Groundwater*, 56 (2017) 288–299.
- [50] J.E. Doherty, M.N. Fienen, R.J. Hunt, Approaches to Highly Parameterized Inversion: pilot-Point Theory, Guidelines, and Research Directions, U.S. Geological Survey Scientific Investigations Report 2010–5168, 2010, p. 36.
- [51] M.J. Knowling, A.D. Werner, D. Herckenrath, Quantifying climate and pumping contributions to aquifer depletion using a highly parameterised groundwater model: Uley South Basin (South Australia), *J. Hydrol.*, 523 (2015) 515–530.
- [52] W.W. Woessner, M.P. Anderson, Selecting Calibration Values and Formulating Calibration Targets for Groundwater Flow Simulations, IAHS Publ. 195: Columbus, Ohio, USA, 1992, pp. 199–212.
- [53] M.C. Hill, C.R. Tiedeman, Effective Groundwater Model Calibration–With Analysis of Data, Sensitivities, Predictions, and Uncertainty, John Wiley & Sons, Inc., Hoboken, N.J., 2007, p. 455.
- [54] C. Zheng, M. Hill, G. Cao, R. Ma, MT3DMS: Model use, calibration, and validation, *Trans. ASABE*, 55 (2012) 1549–1559.
- [55] P.A. Domenico, F. Schwartz, Physical and Chemical Hydrogeology, Wiley, New York, 1998.
- [56] G. Drličková, M. Vaculík, P. Matejkovič, A. Lux, Bioavailability and toxicity of arsenic in maize grown in contaminated soils, *Bull. Environ. Contam. Toxicol.*, 91 (2013) 235–239.
- [57] S. Sharma, I. Kaur, A.K. Nagpal, Estimation of arsenic, manganese and iron in mustard seeds, maize grains, groundwater and associated human health risks in Ropar wetland, Punjab, India, and its adjoining areas, *Environ. Monit. Assess.*, 190 (2018) 384–399.
- [58] J.J. Alava, W.W.L. Cheung, P.S. Ross, U.R. Sumaila, Climate change–contaminant interactions in marine food webs: toward a conceptual framework, *Global Change Biol.*, 23 (2017) 3984–4001.
- [59] C. Su, S. Song, Y. Lu, S. Liu, J.P. Giesy, D. Chen, A. Jenkins, A.J. Sweetman, B. Yvette, Potential effects of changes in climate and emissions on distribution and fate of perfluorooctane sulfonate in the Bohai Rim, China, *Sci. Total Environ.*, 613 (2018) 352–360.
- [60] C.E. Schubert, Groundwater Flow Paths and Travel Time to Three Small Embayments within the Peconic Estuary, Eastern Suffolk County, New York, U.S. Geological Survey Open-File Report 98–4181, 1999.

Supplementary information

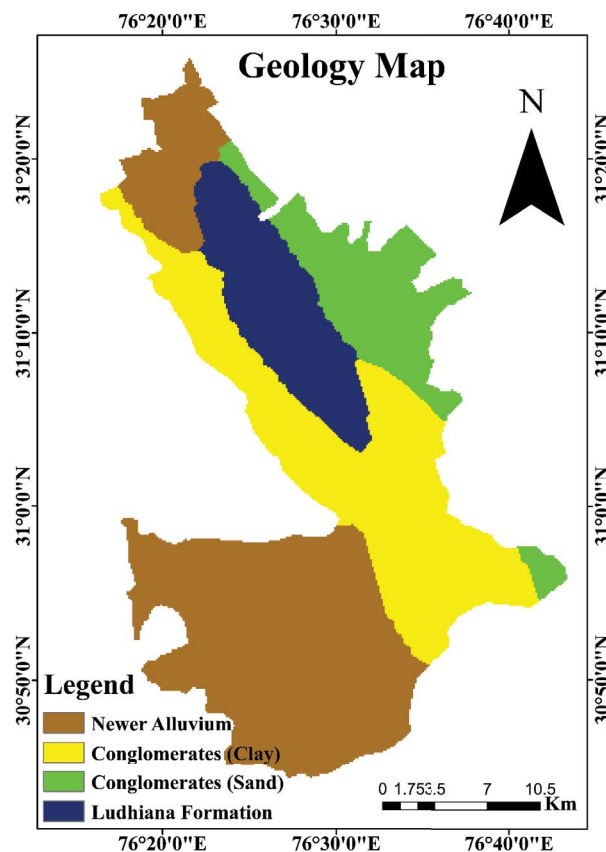


Fig. S1. Geology map of the study region.

Table S1
Sources and observation wells location used in the study

S. No.	Nomenclature used	Sources/observation wells name	Longitude	Latitude
1.	PS1	National Fertilizers Limited (NFL), Naya Nangal	76.365	31.376
2.	PS2	Punjab Alkalis & Chemicals Limited (PACL), Naya Nangal	76.343	31.355
3.	PS3	Ropar Thermal Power Plant (RTPP)	76.583	31.041
4.	PS4	Ambuja Cement Factory (ACF)	76.570	31.040
5.	PS5	Sewage Treatment Plant (STP) Sadabarat, Ropar	76.526	30.982
6.	PS6	STP Badi Haveli, Ropar	76.549	30.900
7.	PS7	STP Rasoolpur, Ropar	76.498	30.844
8.	PS8	STP BBMB, Naya Nangal	76.371	31.399
9.	PS9	STP, Naya Nangal	76.355	31.388
10.	PS10	STP, Anandpur Sahib	76.505	31.241
11.	OW1	Ahmedpur	76.570	31.010
12.	OW2	Bara Chauntha	76.463	30.920
13.	OW3	Bhalan	76.380	31.270
14.	OW4	Brahampur	76.400	31.330
15.	OW5	Chak Dera	76.530	31.040
16.	OW6	Dhair	76.450	31.270
17.	OW7	Dumewal	76.420	31.210
18.	OW8	Hardo Namoh	76.590	31.160
19.	OW9	Kakrali	76.520	30.840
20.	OW10	Nurpur Bedi	76.480	31.170
21.	OW11	Ropar	76.520	30.970
22.	OW12	Saijowal	76.320	31.340
23.	OW13	Singha	76.580	31.020
24.	OW14	Soara	76.390	31.250
25.	OW15	Bhainsa	76.525	31.133
26.	OW16	Purkhali	76.630	30.930
27.	OW17	Salempur	76.463	30.872

PS: Point source; OW: observation well.